Development 140, 2904-2916 (2013) doi:10.1242/dev.092817

The miR-310/13 cluster antagonizes β-catenin function in the regulation of germ and somatic cell differentiation in the *Drosophila* testis

Raluca Pancratov[1,*], Felix Peng[1,*], Peter Smibert[2], Jr-Shiuan Yang[2], Emily Ruth Olson[1], Ciaran Guha-Gilford[1], Amol J. Kapoor[1], Feng-Xia Liang[3], Eric C. Lai[2], Maria Sol Flaherty[1,4,‡] and Ramanuj DasGupta[1,‡]

SUMMARY

MicroRNAs (miRNAs) are regulators of global gene expression and function in a broad range of biological processes. Recent studies have suggested that miRNAs can function as tumor suppressors or oncogenes by modulating the activities of evolutionarily conserved signaling pathways that are commonly dysregulated in cancer. We report the identification of the miR-310 to miR-313 (miR-310/13) cluster as a novel antagonist of Wingless (*Drosophila* Wnt) pathway activity in a functional screen for *Drosophila* miRNAs. We demonstrate that miR-310/13 can modulate Armadillo (Arm; *Drosophila* β-catenin) expression and activity by directly targeting the 3′-UTRs of *arm* and *pangolin* (*Drosophila* TCF) *in vivo*. Notably, the miR-310/13-deficient flies exhibit abnormal germ and somatic cell differentiation in the male gonad, which can be rescued by reducing Arm protein levels or activity. Our results implicate a previously unrecognized function for miR-310/13 in dampening the activity of Arm in early somatic and germline progenitor cells, whereby inappropriate/sustained activation of Arm-mediated signaling or cell adhesion may impact normal differentiation in the *Drosophila* male gonad.

KEY WORDS: Armadillo, Beta-catenin, Wingless, MicroRNA, Stem cells

INTRODUCTION

MicroRNAs (miRNAs) are an abundant class of small, non-coding RNAs that function as global regulators of gene expression (Bushati and Cohen, 2007). At the molecular level, they act by complementary base pairing between the 3′ untranslated region (3′-UTR) or coding sequence of target mRNAs and a 'seed sequence' in the miRNA (Hutvagner and Zamore, 2002; Martinez and Tuschl, 2004; Schnall-Levin et al., 2010). Mutations or misexpression of miRNAs strongly correlate with various human cancers, supporting the notion that they may function as tumor suppressors and oncogenes (Calin and Croce, 2006). miRNAs have also been shown to repress the expression of important cancer-related genes that encode key members of signaling pathways (Croce, 2009). The activity of these pathways might be particularly susceptible to miRNA control as they are subject to multiple levels of regulation leading to specific, dose-dependent phenotypes. We hypothesized that miRNAs might influence oncogenic processes by regulating the activity of crucial signaling pathways that are dysregulated in human cancers.

The evolutionarily conserved Wnt/Wingless (Wg) pathway is one of the most prevalent cancer-associated and developmentally important signaling pathways (Nusse, 2005; Polakis, 2000). A crucial effector of the Wnt pathway is β-catenin (β-cat), or *armadillo* (*arm*) in *Drosophila*. Its functions are highly conserved as a nuclear transcription factor and as a key component of E-cadherin (E-cad)-mediated cell-cell adherens junctions (AJs) (Cox et al., 1996; Hülsken et al., 1994). In the absence of the Wnt signal, a destruction complex (DC) composed of the scaffold protein Axin and other modulators targets β-cat for ubiquitin proteasome-mediated degradation. Stimulation of the pathway by Wnt ligands activates a signal transduction cascade that inhibits DC function. Consequently, β-cat accumulates in the cytosol and translocates into the nucleus, where it activates transcription of target genes together with the Lymphoid enhancer factor (LEF)/T-cell factor (TCF) family of transcription factors, Bcl9 and Pygopus (Hoffmans et al., 2005).

Small variations in cellular β-cat levels have been suggested to have a significant impact on cellular responses by modulating either transcriptional targets or cell adhesion (Goentoro and Kirschner, 2009). We speculated that the fine-tuning of β-cat activity might be subject to miRNA regulation. Although selected miRNAs have been shown to be capable of modulating the Wnt/Wg pathway (Kennell et al., 2008; Saydam et al., 2009; Silver et al., 2007; Thatcher et al., 2008), a comprehensive assessment of miRNAs specifically targeting the nuclear β-cat transcriptional complex has not been attempted. Here, we report a targeted screen to identify specific miRNA modulators of *arm*. We report the identification and characterization of the miR-310/13 cluster (which encompasses miR-310 to miR-313) as a novel antagonist of the Wg pathway that directly targets *arm* and/or *pangolin* (*pan*, or *dTCF*) 3′-UTRs. Importantly, the miR-310/13 loss-of-function (LOF) phenotype *in vivo* is consistent with increased Arm activity and reveals a novel role for miRNA-mediated regulation of Arm/Pan in the normal proliferation and differentiation of early germ and somatic progenitor cells in the *Drosophila* testis.

[1]New York University Langone Medical Center, Department of Pharmacology and the NYU Cancer Institute, 522 First Avenue, SRB #1211, New York, NY 10016, USA. [2]Sloan-Kettering Institute, Department of Developmental Biology, 1275 York Avenue Box 252, New York, NY 10065, USA. [3]New York University Langone Medical Center, Office of Collaborative Science, Microscopy Core, 550 First Avenue, New York, NY 10016, USA. [4]City University of New York, New York City College of Technology, Biological Sciences Department, 300 Jay Street, Brooklyn, NY 11201, USA.

*These authors contributed equally to this work
‡Authors for correspondence (mariasol.flaherty@nyumc.org; ramanuj.dasgupta@nyumc.org)

Accepted 12 May 2013

MATERIALS AND METHODS

Cell culture and high-throughput screen (HTS)

For the HTS, the Wg pathway was activated in *Drosophila* Clone 8 (Cl8) and S2R+ cells [grown as described by DasGupta et al. (DasGupta et al., 2005)] by introducing *Axin* double-stranded RNA (dsRNA), which resulted in a robust, ligand-independent activation of the Wg-responsive dTF12 reporter (DasGupta et al., 2005) (Fig. 1A). We screened a library of miRNA expression constructs [UAS-dsRED-pri-miR (Silver et al., 2007)] that consisted of 75 previously screened pri-miR constructs (Silver et al., 2007) plus 115 as yet unscreened pri-miR plasmids for their ability to suppress dTF12 activity downstream of the DC in this transcriptionally sensitized background. A total of 190 screen-ready plasmids were plated using a Janus MDT automated workstation (Perkin Elmer) in 5 μl aliquots as quadruplicates arranged in a quadrant on a set of three 384-well plates. Several quadrants of four replica wells were left empty for the addition of assay-specific controls. *Axin* dsRNA was generated using the Megascript kit (Applied Biosystems) using the following primers (5′-3′): forward TAATACGACTCACTATAGGGagaccaaacgccgcaccgctcgcc and reverse TAATACGACTCACTATAGGGagacaaaagccggtcgcccgtac (capital letters denote priming regions for T7 RNA polymerase).

Cells were suspended at 20,000 cells/well for S2/S2R+ and 40,000 cells/well for Cl8. The dTF12-luciferase (TOP12-Ffl) reporter and Pol III-Renilla luciferase (PolIII-RL) were utilized as described (DasGupta et al., 2005), with the addition of 0.01 μg actin-GAL4 and 0.1 μg *Axin* dsRNA, and transfected using the Effectene kit (Qiagen). Cells were incubated post-transfection for 5 days and luciferase levels assessed using the Promega Dual-Glo kit (Promega).

For screen data analysis, Firefly luciferase activity values were normalized to those of Renilla luciferase for each replicate. Each plate contained multiple wells treated with empty vector control (pAct or pUASt) and with *arm* and *pan* dsRNA and the dynamic range was consistent with previous observations (DasGupta et al., 2005). Each screen data point was converted to a log score value using the following formula: log score (miR-X) = $\log[N_{exp(X)}/N_{plate\ median}]$. Thus, the obtained log scores could be compared among several plates and different cell lines. The log scores were subjected to uncentered correlation metric cluster analysis using Gene Cluster 3.0 (http://bonsai.hgc.jp/~mdehoon/software/cluster/software.htm) and MatLab (MathWorks).

Drosophila stocks and genetics

Transgenic flies were obtained from BestGene using *P*-element insertion of UAS-dsRED–miR-310/313 (UAS-miR-310/13). The following stocks were obtained from the Bloomington *Drosophila* Stock Center: C96-GAL4, ptc-GAL4, UAS-AxinGFP, UAS-Arm*S10, c587-GAL4, UAS-AxinGFP. UAS-RNAi lines were obtained from the Transgenic RNAi Project (TRiP) at Harvard Medical School.

The mosaic analysis with a repressible cell marker (MARCM) technique (Lee and Luo, 2001) was utilized to generate *Axin* null clones overexpressing either the control UAS-GFP transgene alone or together with UAS-miR-310/13. $Axin^{S044230}$ FRT82 flies were obtained from Nicholas Tolwinski (Tolwinski et al., 2003). Hsflp, tub-GAL4 UAS-GFP;; FRT82, tubGAL80, CD2/TM6c flies for MARCM experiments and Wg-lacZ flies were a gift from Jessica Treisman (New York University School of Medicine). GMR-GAL4 UAS-Wg flies were obtained from Ken Cadigan (University of Michigan, Ann Arbor). Arm* overexpression clones were generated by heat shocking flies expressing actin >STOP>GAL4 UAS-GFP and UAS-miR-310/13 and/or UAS-Arm*, hsflpMKRS/TM6c. For the MARCM experiments, larvae were heat shocked 48-72 hours after egg lay (AEL) at 38°C for 60 minutes. For the flip-out experiments, flies were heat shocked 120 hours AEL at 38°C for 20 minutes.

GFP control and miR-312 GFP sensor flies were obtained from Paul Macdonald (Reich et al., 2009). Flies expressing a short/long *mir-310-313*-encompassing fragment inserted in the attP1 sites were obtained from Eric Lai (Memorial Sloan-Kettering Cancer Center, New York). UAS-Arm RNAi, UAS-E-cad RNAi and UAS-Pan RNAi were obtained from DRSC (TRiP). Bam-GFP flies were generated by the McKearin laboratory (Chen and McKearin, 2003). The d59 deletion stock was generated using *P*-element imprecise excision. Forward primer GAACCCAATTTC-ACACCTCTT and reverse primer CACCAAAGTGCACAGATTGA were utilized in diagnostic PCR to validate the 1 kb deletion in d59 flies.

For fertility analysis, wild-type (WT) females (n=62) were crossed to d59 males (n=44) and eggs were collected on an agar-apple juice plate. Similar egg collection was performed with a WT cross for comparison. Flies were allowed to lay eggs overnight and 200 eggs were collected and incubated at 25°C for 24 hours for each cross. The number of hatched eggs was recorded after the 24-hour incubation, and the above steps were repeated for 7 days. A separate set of crosses was performed similarly that involved crossing d59 females (n=100) to WT males (n=50), compared with a WT cross.

Antibodies and immunostaining

Standard procedures were employed for immunostaining of third instar larval imaginal discs and the *Drosophila* testes. Primary antibodies were diluted in block solution as follows: rabbit anti-RFP (Chemicon) 1:350; guinea pig anti-Senseless (Nolo et al., 2001) 1:1000; mouse anti-β-galactosidase 1:50 [Developmental Studies Hybridoma Bank (DSHB)]; mouse anti-Armadillo 1:200 (DSHB); rabbit anti-cleaved caspase 3 1:200 (Cell Signaling); mouse anti-GFP 1:1000 (Invitrogen); rabbit anti-Vasa 1:1000 (gift of Ruth Lehmann, New York University School of Medicine); guinea pig anti-Tj 1:3000 (gift of Dorothea Godt, University of Toronto); and mouse anti-Eya 1:20 (DSHB). *Drosophila* testes were stained as described (Flaherty et al., 2010). Bright-field and fluorescent images were captured using a Nikon TE2000PFS microscope and Nikon Elements software or using a Zeiss LSM 510 META confocal microscope and Zeiss LSM software versions 4.2 SP1 and Zen. Clonal area quantitation was performed using Nikon Elements and MatLab. Cell perimeter analysis in the *Drosophila* testis was performed using ImageJ (NIH).

DNA constructs

The SV40 promoter of psiCheck-2 (Promega) was excised by digestion with *Bgl*II and *Nhe*I and replaced with the heat shock minimal promoter cloned by DasGupta et al. (DasGupta et al., 2005). *arm* 3′-UTR and *pan* 3′-UTR fragments were cloned into the polylinker site modified by the Eric Lai laboratory using the 5′ *Not*I and 3′ *Xho*I sites. Primers were: *pan*, forward ATAGAATGCGGCCGCCAAGATTCACGCAAGAATTAATTGAC and reverse CCGCTCGAGTGACTGGGTTAAGAACTGGATC; *arm*, forward ATAGAATGCGGCCGCATAGATTCGATGCAGGGTCT and reverse CCGCTCGAGCATATGAAGGGAAATGTACGA.

For the cloning of hsa-miR-25 we utilized the forward GCGGCCGCCATTCTCACACGTGCCTAAG and reverse TCTAGATGAT-TACCCAACCTACTGCT primers to amplify the precursor miR-25 and insert it into the *Not*I and *Xho*I sites of pcDNA3.1(+) (Invitrogen). The genomic DNA utilized was obtained from Applied Biosystems. Human MIR-92a and MIR-18 primary transcript vectors were obtained from Cell Biosciences. The Wnt reporter for mammalian cells was STF16 (DasGupta et al., 2005).

Western blotting

S2R+ cells in 12-well plates were transfected with 60 ng actin-GAL4, 240 ng UAS-miR and 4 μg *Axin* dsRNA using the Effectene kit. Standard PAGE western protocols were used for cell lysis, preparation of extracts, protein quantification and gel electrophoresis. Primary antibody against Arm (N2 7A1 from DSHB) was used at 1:200. Secondary antibodies exhibiting infrared fluorescence with emission wavelengths of 700 and 800 nm were utilized for secondary detection. Detection and quantitation of band intensities were performed using Li-COR Odyssey.

RESULTS

A screen for miRNA modulators of Wg signaling

To identify miRNAs specifically targeting β-cat activity downstream of the DC, we used a *Drosophila* cell-based screening platform developed for the discovery of novel small-molecule inhibitors of the Wnt pathway (Fig. 1A) (see Materials and methods for a detailed screen protocol). The design of the primary screen allowed us to screen for miRNAs which when overexpressed would specifically modulate the activity of a Wnt/β-cat-responsive

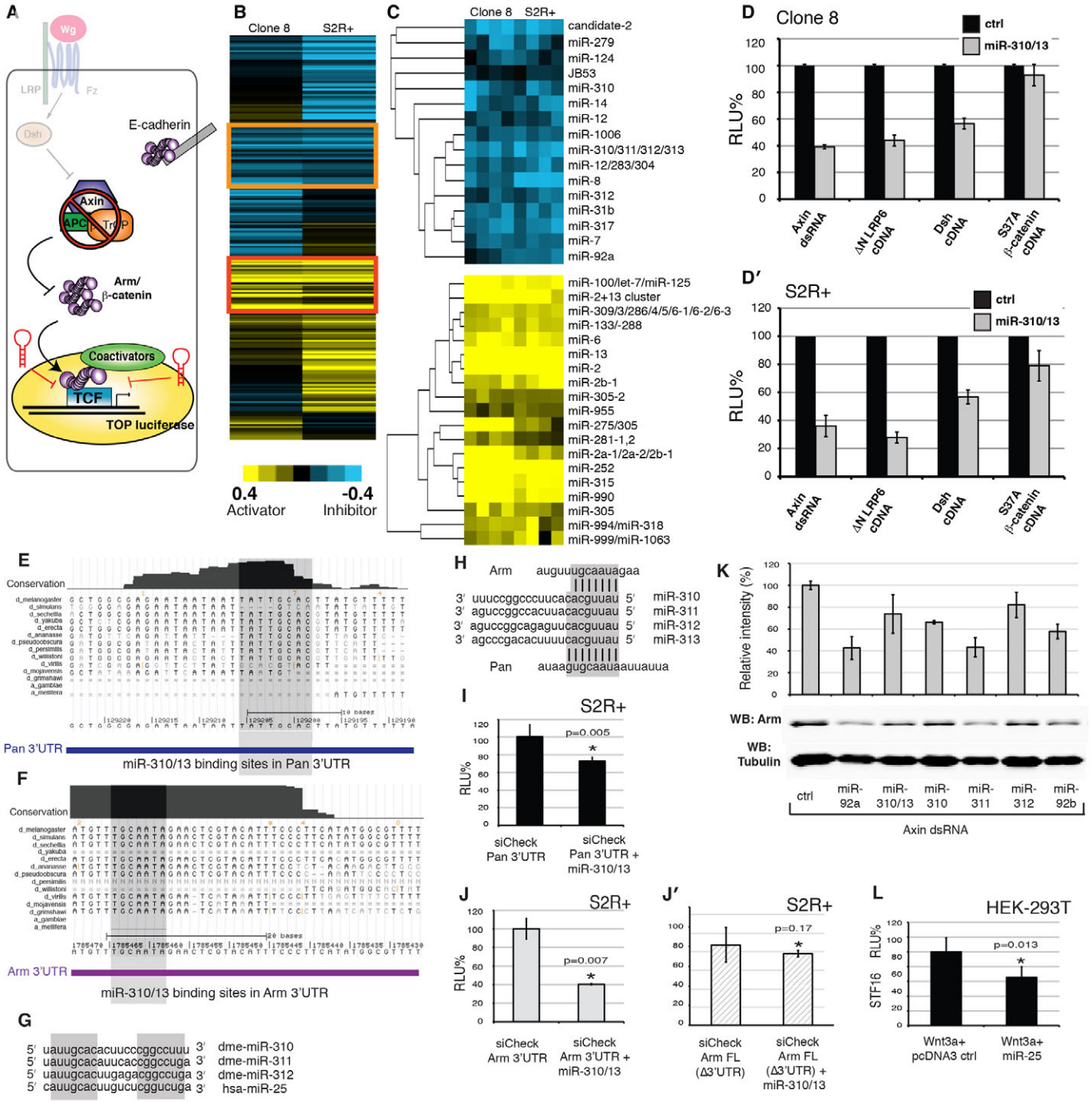

Fig. 1. Identification of miR-310/13 in an RNAi-based targeted screen for miRNAs that suppress Wg pathway activity downstream of Axin. (**A**) The primary screen. miRNAs were tested for their ability to modulate Wg reporter (dTF12) activity in Clone 8 and S2R+ cells, where the pathway was ectopically activated by *Axin* dsRNA. (**B**) Unbiased cluster analysis of averaged log normalized scores for each screened miRNA in Clone 8 and S2R+ cells. (**C**) Highlighted clusters of strong inhibitors of the Wg reporter (top panel; orange box in B), including the previously reported Wg antagonist miR-8. Note the functional clustering of members of the miR-310/13 cluster. Also highlighted are potent activators of the Wg reporter (bottom panel; red box in B), including the previously published Wg agonist miR-315. (**D**,**D′**) Epistasis analyses. miR-310/13 strongly inhibits the dTF12-luciferase reporter when the Wg pathway is activated by dsRNA-mediated knockdown of Axin or by cDNA expression of ΔNLRP6 or Dsh. No significant inhibition by miR-310/13 was observed upon pathway activation with the constitutively active S37Aβ-cat. (**E**) Alignment of mature regions of *Drosophila* miR-310, miR-311, miR-312 and the human ortholog hsa-miR-25. d, *Drosophila*; a, *Anopheles*. (**F**,**G**) Alignments of multiple *arm* (F) and *pan* (G) 3′-UTR transcripts in various *Drosophila* and insect species revealing a conservation of miR-310/13 binding sites in *arm* and *pan* mRNA. (**H**) Predicted binding sites of miR-310/13 components in the 3′-UTR of *arm* and *pan*. (E-H) Gray shading highlights the conserved regions. (**I-J′**) *pan* 3′-UTR (I) and *arm* 3′-UTR (J) containing luciferase sensor reporters are significantly downregulated in the presence of miR-310/13, compared with control sensor containing full-length cDNA of *arm* lacking the 3′-UTR (Δ3′UTR, J′). (**K**) Western blot (WB) showing the ability of the miR-310/13 cluster and its individual components to significantly downregulate levels of Arm protein in S2R+ cells treated with *Axin* dsRNA. (**L**) hsa-miR-25 inhibits Wnt3a-induced activation of the SuperTOPFlash/STF16 reporter in human embryonic kidney (HEK293T) cells. Error bars indicate s.d. (n=4). P-values by Student's t-test. RLU, relative luciferase units.

luciferase reporter gene in cells where the pathway is artificially activated using dsRNA-mediated knockdown of Axin (Fig. 1A).

Primary screen results consisting of control-normalized log scores in quadruplicate for each miRNA (supplementary material Tables S1, S2) were subjected to hierarchical clustering (Fig. 1B,C), which grouped miRNAs into clusters related by similar potency in modulating Wg activity (strong inhibitors in the orange box and strong activators in the red box in Fig. 1B). Corroborating screen robustness, we identified previously characterized miRNA modulators of the pathway, miR-315 (Silver et al., 2007) and miR-8 (Kennell et al., 2008), as potent activators and inhibitors, respectively, of the dTF12 reporter (Fig. 1C). Interestingly, the Wg pathway inhibitor miR-8 functionally clustered together with miR-310, miR-311, miR-312, miR-313 (the miR-310/13 cluster), miR-92a and miR-92b (Fig. 1C). miR-310/13 and miR-92a/b are components of a highly conserved family, with orthologs in mouse (not shown) and human (Fig. 1E) (Tanzer and Stadler, 2004).

Secondary epistasis assays using known components of the Wg pathway confirmed that the miR-310/13 cluster functions downstream of the DC (Fig. 1D,D′). Expression of miR-310/13 strongly inhibited the dTF12 reporter when the pathway was activated by RNAi-mediated knockdown of Axin, by cDNA expression of a constitutively active form of human LRP6 [ΔNLRP (Brennan et al., 2004; DasGupta et al., 2007)] and by cDNA expression of Dsh (DasGupta et al., 2005). By contrast, expression of miR-310/13 failed to significantly inhibit the dTF12 reporter induced by the constitutively active form of β-cat [S37Aβ-cat (Easwaran et al., 1999)], suggesting that it might function upstream or at the level of Arm regulation (Fig. 1D,D′). The human ortholog of the *Drosophila* miR-310/13 cluster, hsa-miR-25 (MIR25) (Fig. 1E,L), was also able to downregulate the Wnt reporter STF16 (DasGupta et al., 2005) in HEK293T cells, suggesting that the function of this miRNA cluster might be evolutionarily conserved. Notably, we also identified hsa-miR-25 as a negative modulator of the STF16 reporter in an independent, unbiased screen for miRNAs that could modulate Wnt signaling in human cells (Anton et al., 2011).

miR-310/13 targets *arm* and *pan* 3′-UTRs

The mature sequences of each individual miRNA of the miR-310/13 cluster are very similar and share identical seed sequences (Fig. 1E), which is suggestive of a set of overlapping targets. Querying the miRNA target prediction algorithms TargetScan and MIRANDA identified highly conserved binding sites for miR-310/13 in the 3′-UTRs of *arm* and *pan* (Fig. 1F-H). To test the functionality of these putative binding sites, we generated luciferase sensors containing the *arm* and *pan* 3′-UTRs. We observed a significant decrease in luciferase levels in the presence of miR-310/13 compared with the control for both constructs (Fig. 1I,J). Importantly, the activity of a control luciferase sensor containing *arm* cDNA (Arm FL) lacking the 3′-UTR and any predicted miR-310/13 binding sites was not affected by miR-310/13 misexpression (Fig. 1J′). Western blots of cells treated with *Axin* dsRNA showed that transfection of the miR-310/13 cluster and its individual members led to a significant decrease in Arm protein levels compared with the control (Fig. 1K).

We speculated that if miR-310/13 was capable of directly modulating Arm levels, then its clonal overexpression should resemble *arm* LOF. We thus generated GFP-marked flip-out (FO) clones expressing miR-310/13 in the wing imaginal disc. Clones lacking wild-type (WT) *arm* are difficult to recover because Arm influences both cell proliferation/growth and cell-cell AJs, and cells delaminate and die in the absence of AJs. Similar observations have been made in LOF clones for components of Wg signaling and Arm-mediated cell adhesion, including *pan*, *arr*, *fz/fz2* and *DE-cad* (*shotgun* – FlyBase) (Peifer et al., 1991; Widmann and Dahmann, 2009). However, $arm^{-/-}$, $arr^{-/-}$ or $DE\text{-}cad^{-/-}$ clones can be forced to survive by expressing p35, an inhibitor of apoptosis. These ‘undead’ cells delaminate and are extruded towards the basal side of the epithelium (Widmann and Dahmann, 2009). Concordantly, clonal populations expressing miR-310/13; UAS-GFP were difficult to recover (Fig. 2B) compared with control UAS-GFP clones (Fig. 2A).

To test whether the toxicity of miR-310/13 is a function of its inhibitory activity on Arm levels, we co-expressed a 3′-UTR-deficient form of activated Arm (Arm^{S10}) (Pai et al., 1997) and observed a significant rescue of FO clone viability (Fig. 2C, quantification in 2D). Furthermore, we were also able to rescue UAS-miR-310/13 FO clones by co-expressing p35, similar to the observations made by Widmann and Dahmann (Widmann and Dahmann, 2009) (compare Fig. 2E″ with 2B). Interestingly, miR-310/13, p35 clones (Fig. 2E″) appeared to be much smaller than WT clones (Fig. 2A). *x-z* sections of these clones revealed that they were composed of very few cells (one to three, as judged by counting nuclei; red and yellow arrowheads in Fig. 2F), and appeared to be delaminating from the epithelial plane (red and white arrowheads in Fig. 2G), suggesting defective proliferation and compromised adhesion. Consistent with the observed phenotype, early clones expressing miR-310/13, p35 displayed reduced Arm expression (Fig. 2H-H″).

Together, these results suggest that the miR-310/13 cluster might directly modulate Arm and/or Pan levels by targeting the 3′-UTRs of their transcripts, thereby influencing their function in cell signaling and adhesion.

Overexpression analysis of the miR-310/13 cluster *in vivo*

We utilized the GAL4-UAS system to drive the expression of miR-310/13 and co-cistronic dsRED in the *Drosophila* leg and wing imaginal discs, and assessed its effect on modulating the endogenous response to Wg signaling (Fig. 3). In the leg disc, Wg signaling in the ventral compartment restricts *dpp* expression to the dorsal leg primordia, as highlighted by Dpp-lacZ staining (Fig. 3) (Estella and Mann, 2008). Antagonizing Wg signaling leads to the derepression and expansion of Dpp in the ventral compartment of the disc (Estella and Mann, 2008; Struhl and Basler, 1993). Consistent with its putative function as an antagonist of Wg signaling, expression of miR-310/13 under *patched* (*ptc*)-GAL4 (indicated by dsRED staining at the anteroposterior boundary of the leg disc; Fig. 3B′) resulted in significant ectopic expression of Dpp-lacZ in the ventral compartment (yellow arrowhead in Fig. 3B″, compare with control in 3A″; additional examples are shown and quantified in supplementary material Fig. S1). Mild expansion of the endogenous expression of Dpp-lacZ was also evident in the dorsal compartment (red arrowheads in Fig. 3A″,B″).

Misexpression of the miR-310/13 cluster along the presumptive wing margin (dorsoventral boundary) of the wing imaginal disc strongly suppressed expression of the Wg target gene *senseless* (*sens*) (Basler and Struhl, 1994), in a manner similar to that observed for known negative regulators such as Axin (Fig. 3C-F). Sens reduction in larval tissues correlated with loss of wing margin sensory bristles and notching of the adult wing (Fig. 3H-I′, compare with WT in 3G,G′). Co-expression of an active form of Arm (Arm*), the transcript of which lacks the endogenous 3′-UTR

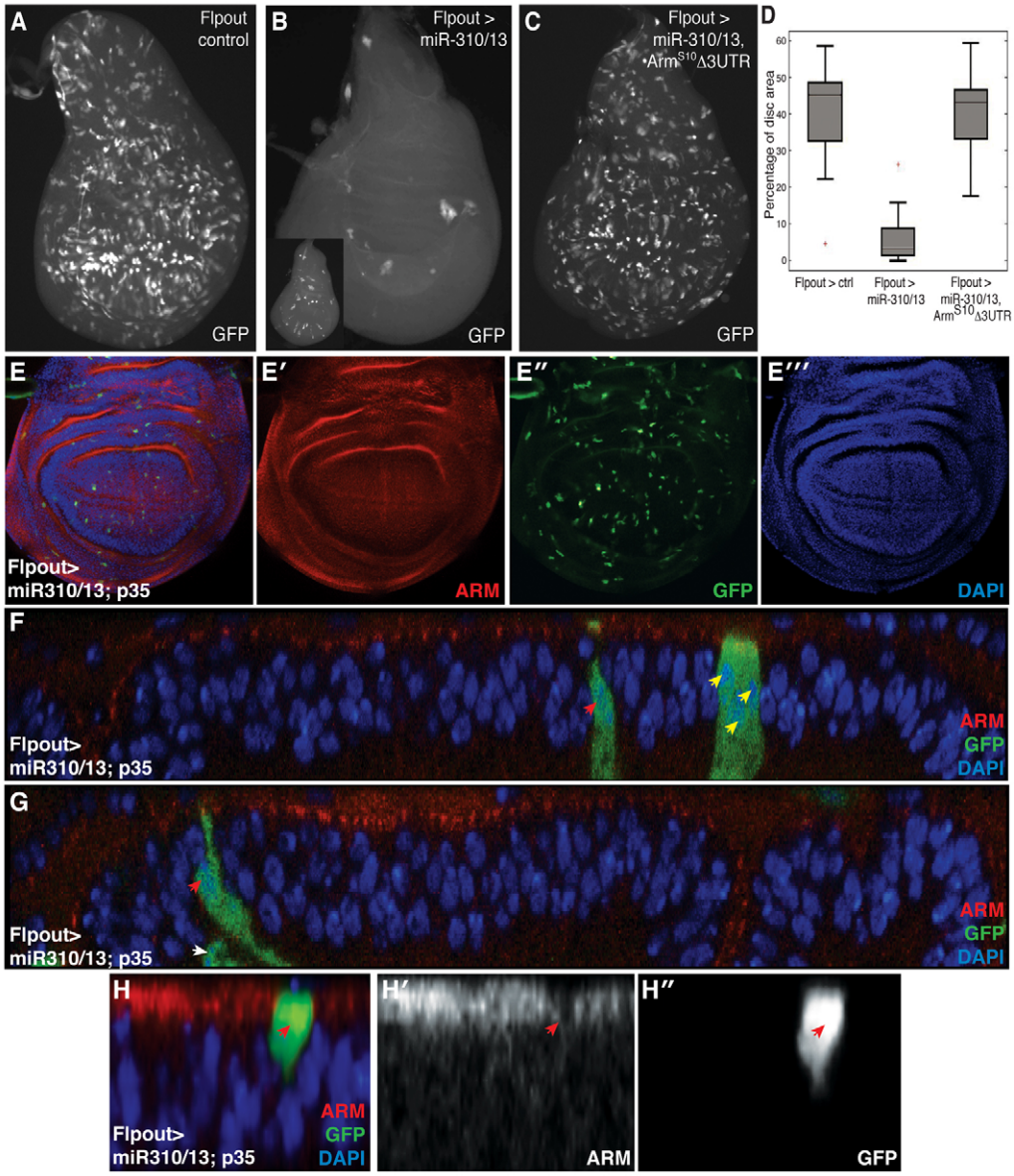

Fig. 2. miR-310/13 flip-out clones mimic loss of Arm activity by downregulating expression of endogenous Arm. (**A-C**) Flip-out (FO) clones ectopically expressing miR-310/13 and GFP are difficult to recover in the wing imaginal disc (B; see range of clone recovery in the inset), compared with control GFP WT clones generated under identical conditions (A). The viability of miR-310/13-expressing GFP^{+} clones is robustly restored upon co-expression of Arm^{S10} lacking the 3′-UTR (C). (**D**) Quantification of data generated in A-C as percentage clone recovery with respect to total disc area. The error bars for minima and maxima for percentage of disc area are indicated. (**E-E‴**) FO clones co-expressing miR-310/13 and p35. Note the recovery of these clones compared with the miR-310/13 FO clones shown in Fig. 1B. (**F**,**G**) *x-z* sections of the UAS-miR-310/13, UAS-p35 FO clones reveal that the recovered clones are small, composed of just one to three cells (red and yellow arrowheads, F), suggesting a failure in proliferation. Cells within the clones also appeared to be delaminating from the epithelial plane (G); red arrowhead indicates a cell at an early stage of delamination, whereas the white arrowhead marks a cell that has completely delaminated from the epithelial plane. This is likely to be due to loss of adhesion upon downregulation of Arm by miR-310/13. (**H-H″**) High-magnification image of an early p35, miR-310/13 FO clone reveals significant reduction of endogenous Arm expression at the cell junctions within the clone (red arrowheads in H′,H″).

(Δ3′UTR), with the miR-310/13 cluster rescued wing notching and the loss of sensory bristles (Fig. 3J), resulting in wings resembling those derived from flies overexpressing Arm* alone (Fig. 3K). Interestingly, closer inspection of the dorsal wing margin bristles revealed that co-expression of miR-310/13 with Arm* inhibited specification of the extra wing margin bristles observed in animals expressing Arm* alone (Fig. 3J′,K′). These observations suggest that miR-310/13 might rescue the Arm* overexpression phenotype by regulating endogenous *pan* activity (Fig. 1G-I), which is required to specify the sensory wing margin bristles by activating Sens (Olson et al., 2011).

Additionally, we used MARCM to assess whether misexpression of miR-310/13 could suppress the ectopic activation of Sens in clones of cells lacking WT Axin (supplementary material Fig. S1). *Axin*$^{-/-}$ cells that express high levels of GFP, signifying robust expression of miR-310/13 (arrows in supplementary material Fig. S1K-M and ratiometric image in S1M′ comparing Sens with GFP), displayed reduced levels of Sens expression compared with control

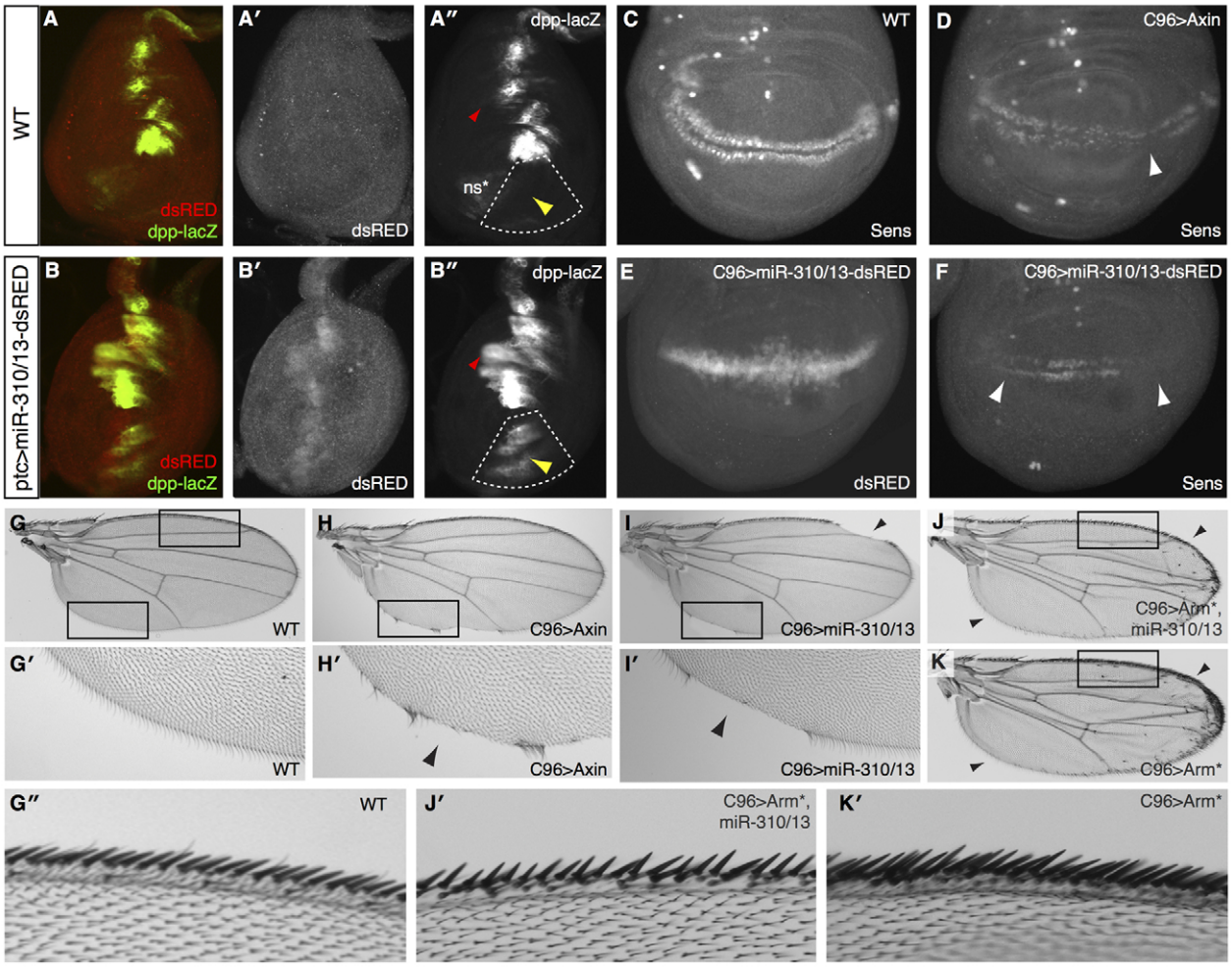

Fig. 3. Overexpression of the miR-310/13 cluster in *Drosophila* imaginal discs phenocopies Wg loss of function. (**A-A″**) Dpp-lacZ expression is restricted by Wg to the dorsal compartment of WT *Drosophila* leg discs (yellow arrowhead in A″). ns*, non-specific staining. (**B-B″**) Misexpression of miR-310/13-dsRED using ptc-GAL4 leads to Dpp-lacZ derepression and expansion to the ventral compartment of the leg disc (yellow arrowhead in B″; quantified in supplementary material Fig. S2). Note the expression of miR-310/13 in the *ptc* expression domain, visualized by dsRED expression in B′. Red arrowheads (A″,B″) indicate mild expansion of the endogenous expression of Dpp-lacZ evident in the dorsal compartment. (**C-I′**) Effect of misexpression of miR-310/13 on *sens*, a Wg target gene, and wing patterning/growth of the wing imaginal disc. Sens is expressed in two rows at the dorsoventral boundary of the wing disc and is used as a readout for Wg signaling activity (C). C96-GAL4-driven expression of Axin leads to downregulation of Sens (D, arrowhead), adult wing notching, and depletion of sensory bristles (H,H′, black arrowhead), compared with the WT control (C,G,G′). Misexpression of miR-310/13-dsRED in the C96 domain (note dsRED expression in E) phenocopies Axin overexpression, both in its ability to repress Sens (F, arrowheads) and by causing wing notching in the adult (I,I′, black arrowheads). (**J**,**K**) Co-expression of *arm* lacking a 3′-UTR together with miR-310/13 leads to significant rescue of wing notching and bristle loss, in addition to the formation of ectopic sensory bristles (J) similar to those observed in flies overexpressing Arm alone under C96-GAL4 (K). (**G″**,**J′**,**K′**) Magnification of dorsal wing margins from WT flies (G″), flies that co-express an active form of Arm (Arm*) and miR-310/13 (J′), and those expressing Arm* alone (K′). Note that the increase in dorsal sensory wing margin bristles in flies expressing Arm* alone (K′) is rescued by the co-expression of miR-310/13 (J′). Boxes indicate the regions magnified.

clones not expressing miR-310/13 (arrows in supplementary material Fig. S1I,J).

These data confirm our hypothesis that the miR-310/13 cluster functions downstream of the DC, most likely at the level of nuclear transcription. Our results also indicate that misexpression of miR-310/13 *in vivo* can phenocopy the loss of Arm/Wg signaling activity, both in wing and leg imaginal discs.

Loss-of-function analysis of miR-310/13

To explore the physiological function of the miR-310/13 cluster in *Drosophila*, we generated a deletion mutant (d59) by *P*-element-mediated imprecise excision of a 1.1 kb fragment encompassing the pri-miR-310/13 coding region (supplementary material Fig. S2A,B). d59 homozygous (d59/d59) mutant animals were viable and lacked any conspicuous defects, similar to what has been reported by Tsurudome et al. (Tsurudome et al., 2010) for independently generated deletion mutants of the *mir-310-313* locus. However, closer inspection revealed that less than 3% of over 200 counted eggs laid by d59/d59 flies hatched and developed into adults, while the majority of the eggs appeared unfertilized (data not shown). We tested whether this sterility phenotype was gender associated by measuring the hatching rate of the eggs laid following crossing of d59/d59 females or males to WT counterparts, as compared with the hatching rate of eggs from a purely WT cross

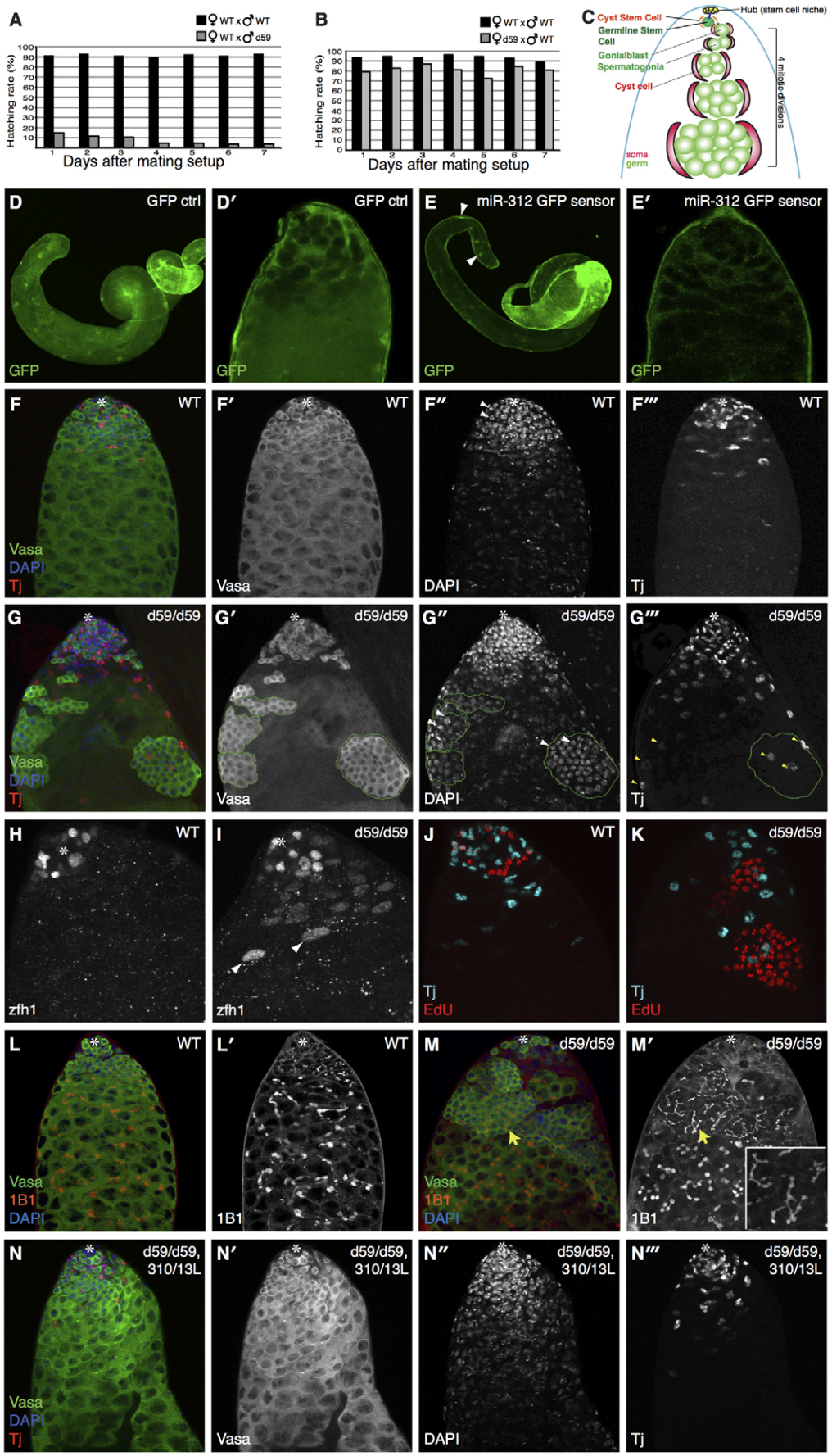

Fig. 4. See next page for legend.

Fig. 4. miR-310/13 null flies (d59/d59) exhibit a male-specific fertility defect. (**A**,**B**) d59/d59 males exhibit severe sterility. Hatching rate of eggs laid by d59/d59 males (*n*=200) crossed to WT females is significantly decreased (gray bars) compared with a WT control cross (black bars) (A). d59/d59 females exhibit no significant fertility defect (B). (**C**) Model of WT testes (see text for details). (**E**,**E′**) GFP sensor containing multimerized miR-312 binding sites displays a marked reduction of the GFP signal in the apical and medial domain of the testis, but not in the nuclei of the muscle sheath cells (arrowheads in E; see quantification of GFP sensor fluorescence intensity in supplementary material Fig. S2I-K). (**D**,**D′**) Note that there is increased cytoplasmic GFP expression in both soma and germ in the control testis. However, we consistently see much weaker GFP expression in germ cells compared with soma. (**F-F‴**) WT testis showing the germline marker Vasa in green, DAPI in blue, and the CySCs/early somatic cyst cell marker Tj in red. (**G-G‴**) Testes of d59/d59 flies exhibit abnormal accumulations of early germ cells and somatic cyst cells. The germ cell clusters (outlined by green dashed line in G′-G‴) accumulate further away from the hub compared with WT control. The cells within these clusters display condensed nuclear morphology, as shown by DAPI staining (arrowheads in G″) and appear to be poorly differentiated. The germ cell clusters are almost always associated with ectopic Tj^+ cells (G,G‴), which show a marked increase in number compared with WT (compare G‴ with F‴). (**H**,**I**) Ectopic cyst somatic cells are positive for the CySC/early cyst cell marker Zfh1 in d59 mutant testes (I), compared with WT (H). Note that the bright $Zfh1^+$ cells (arrowheads in I) are associated with germ cell clusters (shown in the merge in supplementary material Fig. S2M). (**J**,**K**) Synchronous cell division in abnormal germ cell clusters in d59/d59 testes (K), compared with WT (J), as revealed by EdU staining. (**L-M′**) Abnormal germ cell accumulations in d59 homozygous testes harbor branched fusomes (M′). 1B1 marks fusomes (red) (L,M). GSCs contain 'dot' fusomes, and the degree of fusome branching in germ cells correlates with the extent of differentiation (L,L′). miR-310/13-deleted testes display extensive branched fusomes within abnormal germ cell clusters (yellow arrows in M,M′; higher magnification in M′ inset). (**N-N‴**) Rescue of the germ cell accumulation phenotype in d59/d59 males expressing a genomic construct spanning the *mir-310-313* locus as well as a region upstream of the transcription start site (miR-310/13L). Asterisks mark the hub.

(Fig. 4). Embryos deposited by d59/d59 mothers hatched at only a slightly lower rate than WT embryos (Fig. 4B). By contrast, d59/d59 males appeared to have severe fertility defects, with significantly lower hatching rates of their progeny compared with eggs fertilized by WT males (Fig. 4A).

Since d59/d59 males displayed a sterility phenotype, we explored whether the miR-310/13 cluster was expressed in the *Drosophila* testis (Fig. 4D-E′). Examination of testes of miR-310/13 sensor flies expressing tubulin-GAL4>UAS-GFP flanked by hexamerized binding sites for miR-312 (Reich et al., 2009) revealed markedly lower GFP levels (Fig. 4E,E′) compared with control sensor flies that express GFP lacking miR-312 binding sites (Fig. 4D,D′; quantification in supplementary material Fig. S2I-K). These results indicate that the miR-310/13 cluster, all components of which share a common seed sequence, is expressed and functional in the *Drosophila* testis. Importantly, this sensor did not appear to be downregulated in other tissues such as larval imaginal discs (data not shown), which could explain the lack of any discernible phenotypes in adult appendages or imaginal discs of d59/d59 animals (data not shown).

The stem cell niche of the *Drosophila* testis, called the hub, resides at the apical tip and secretes the self-renewal signal Unpaired to adjacent germline stem cells (GSCs) and somatic cyst stem cells (CySCs) (Kiger and Fuller, 2001; Morrison and Spradling, 2008; Tulina and Matunis, 2001). GSCs divide asymmetrically, generating another GSC that remains at the hub and a daughter gonialblast (GB) that is enveloped by two somatic cyst cells (Fig. 4C). Whereas somatic cells undergo one round of division (Lindsley and Tokuyasu, 1980), dividing GBs divide four times to form a cyst of 16 spermatogonial cells, which undergo meiosis and eventually differentiate into spermatocytes (Fig. 4C). Dividing germ cells do not undergo complete cytokinesis, but are linked by actin-rich cytoskeletal structures called fusomes (Lin et al., 1994). It has been shown that the interactions between somatic cyst cells and germ cells are crucial for a proper differentiation program (DiNardo et al., 2011; Flaherty et al., 2010; Issigonis and Matunis, 2012; Leatherman and DiNardo, 2008; Lim and Fuller, 2012). Understanding the exact mechanisms of this signaling crosstalk remains an area of active study.

Consistent with the observed sterility, testes of d59/d59 males exhibited abnormal accumulations of what appeared to be large cysts of overproliferating, undifferentiated spermatogonia/germ cell clusters (germ cells are marked by *vasa* in Fig. 4G-G‴). These clusters (within green dashed lines in Fig. 4G,G′) resided far from the hub, and the number of germ cells within each cluster far exceed (>16) those found within normally differentiating WT germline cysts (Fig. 4F′) (see the testis phenotype modeled in Fig. 6B). There was also a marked increase in the number of somatic cyst cells, as evident by an excess of cells positive for Traffic jam (Tj), a CySC/early cyst marker (Li et al., 2003), in d59/d59 testes that resided far from the hub (compare Fig. 4G‴ with 4F‴). A majority of these cyst cells also expressed Zn finger homeodomain 1 (Zfh1), a marker that is predominantly expressed in CySCs and at lower levels in early cyst progenitors (Fig. 4I, compare with WT control in 4H; supplementary material Fig. S2F; *n*=28) (Leatherman and DiNardo, 2008). Moreover, most of the $Zfh1^+$ cells did not express the cyst differentiation marker Eyes absent (Eya) (white arrowheads in supplementary material Fig. S2F), thereby suggesting a specific expansion of early cyst cells in testis lacking miR-310/13 function. That said, some cyst cells co-expressed Zfh1 and low levels of Eya, indicating that some of these cells can also differentiate (yellow arrowheads in supplementary material Fig. S2F; *n*=19). Interestingly, the abnormal germ cell clusters in the d59/d59 testis were found to typically associate with at least two or more Tj^+ cyst cells (yellow arrowheads in Fig. 4G‴), which in many cases also expressed Zfh1 (arrowheads in Fig. 4I; supplementary material Fig. S2F,M; 22 of 28 analyzed testes). However, some of the germ cell clusters associated with the $Zfh1^+$ cyst cells were also found to be engulfed by Eya^+ cyst cells (red arrowheads in supplementary material Fig. S2F; *n*=19). Nonetheless, these observations suggested that the increased numbers of $Zfh1^+$ CySC/early cyst cells could be inhibiting differentiation in the associated clusters of germ cells, thereby resulting in the accumulation of large undifferentiated germ cell cysts in d59/d59 testis.

Concordant with our hypothesis that the increased $Zfh1^+$ cyst cells could be inhibiting differentiation in the germ lineage, the expression of the differentiation marker Bag of marbles (Bam) in the large germ cell clusters was either low or undetectable in the d59/d59 testes (arrowheads in supplementary material Fig. S2H,H′) (McKearin and Spradling, 1990). Bam protein expression in these clusters was similar to that typically observed in early, undifferentiated germ cells in WT testes (compare Bam staining in d59 mutants versus WT, supplementary material Fig. S2H,H′ versus S2G,G′) (Insco et al., 2009), suggesting that they fail to undergo normal differentiation and instead might go through an increased number of transit amplifying (TA) divisions. Indeed, EdU staining

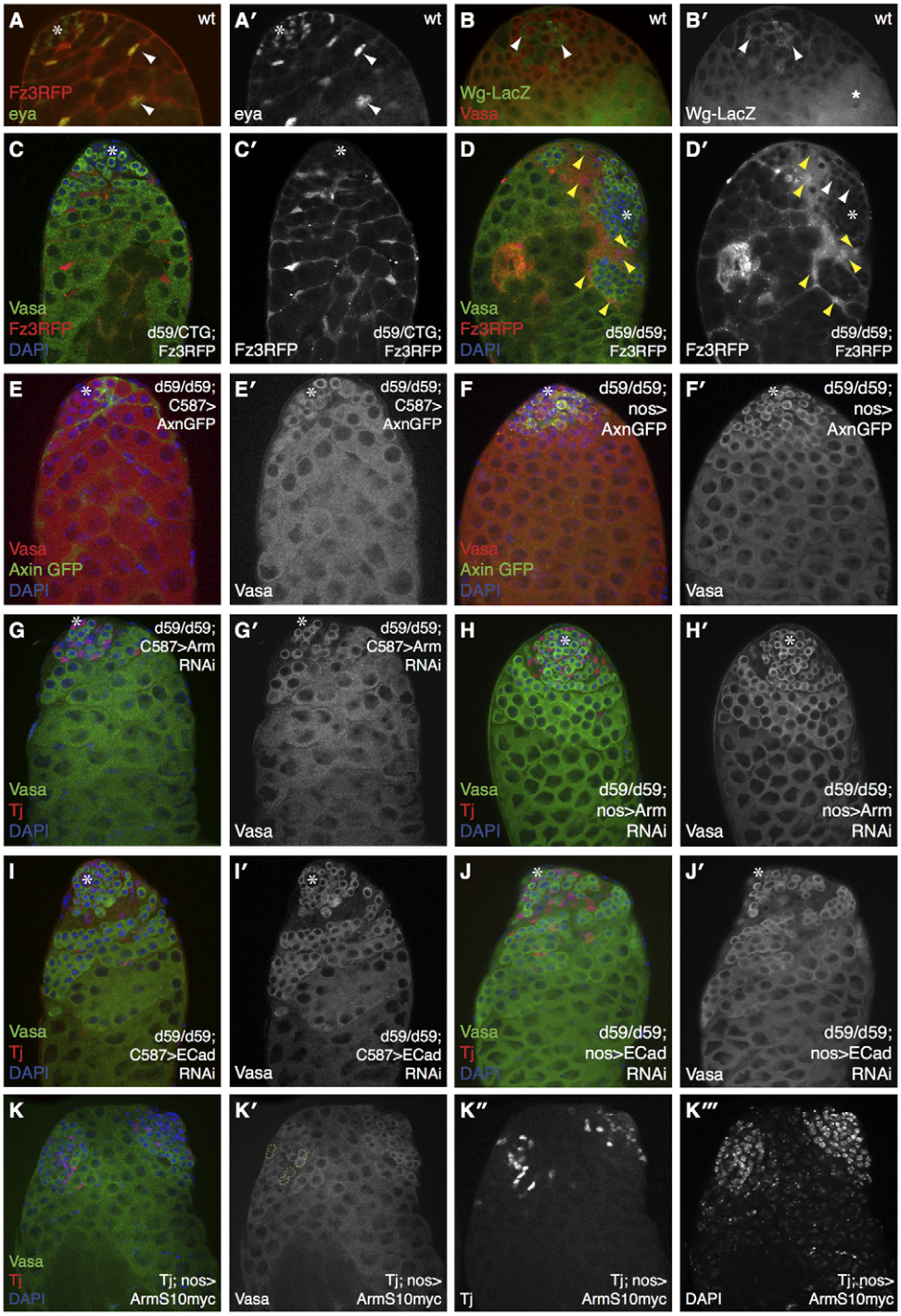

Fig. 5. Interfering with Arm activity and cell junctions in both somatic and germ cells rescues the abnormally differentiated germ cell clusters in d59 homozygous testes. (**A**,**A′**) Fz3RFP (Wg reporter) expression is restricted to cells of the somatic lineage as marked by *eya*. (**B**,**B′**) Wg-lacZ expression is increased in CySCs and their early progeny (arrowheads) proximal to the hub, indicating that Wg signaling may be active in these cells. Star marks non-specific staining. (**C**,**C′**) d59/CyO-Twist-GFP (CTG); Fz3RFP reporter testes exhibit normal morphology of germ cells (Vasa^{+} cells). (**D**,**D′**) d59/d59; Fz3RFP testes exhibit both a stronger RFP signal and an expansion in the domain expressing Fz3RFP reporter (D′). Yellow arrowheads indicate Fz3RFP, Tj^{+} cells. Ectopic RFP expression is seen in germ cells (white arrowheads, D′). (**E-J′**) Rescue of the germ and somatic cell accumulation phenotype in d59/d59 flies upon overexpression of Axin using the soma-specific C587-GAL4 driver (E,E′) or upon RNAi-mediated depletion of Arm (G,G′) and a partial rescue upon RNAi-knockdown of E-cad (I,I′) in the soma. Similar observations were made with germline expression of Axin (F,F′) or short hairpins against *arm* (H,H′) and *E-cad* (J,J′). Note the reappearance of properly differentiating germ cell clusters and normal nuclear morphology in each rescue example. (**K-K‴**) Overexpression of Arm in both germ (nos-GAL4) and somatic (Tj-GAL4) cells resulted in the formation of ectopic germ cell clusters (K′,K‴) associated with a distinct set of Tj^{+} cells (K″). Ectopic two-cell clusters in K′ are marked by the dashed yellow line. Asterisks mark the hub.

revealed that the germ cells in these abnormal clusters continue to proliferate synchronously (Fig. 4K, compared with WT in 4J; *n*=32). Moreover, 1B1 (Hu li tai shao – FlyBase) staining showed that the germ cells within each cluster are connected by a shared cytoplasm, as evidenced by the presence of large branched fusomes as opposed to the ‘dot’ fusomes characteristic of GSCs and GBs (Fig. 4L-M′) (Lin et al., 1994).

Based on the condensed nuclear morphology of spermatogonial cells within the large ectopic germ cell clusters (see DAPI staining in Fig. 4G″, white arrowheads, compared with the early germ cells in WT testis in 4F″), the proliferation status (Fig. 4K), the presence of branched fusomes (Fig. 4M′) and their inability to activate the differentiation program (supplementary material Fig. S2H,H′), we conclude that the spermatogonial cells within these clusters represent early germ cell progenitors but are distinct from GSCs/GBs. Importantly, the d59/d59 testes phenotype could be rescued by reintroducing a large genomic construct spanning the *mir-310-313* region (miR-310/13L), indicating that the observed phenotype was specific to the loss of miR-310/13 function (Fig. 4N-N‴).

Reduction of Wg/Arm activity rescues the miR-310/13 LOF phenotype

Although the *Drosophila* testis is a well-studied model system for stem cell maintenance, little is known about the contribution of Wg

signaling to this process. Recent evidence has highlighted important functions of E-cad and Arm: GSCs require E-cad for their attachment to the hub and to ensure asymmetric cell division, thus maintaining self-renewal ability (Leatherman and DiNardo, 2008; Leatherman and DiNardo, 2010). Moreover, Arm binds E-cad at AJs and is highly expressed in the hub, which might suggest important functions for Arm-mediated cell adhesion in stem cell homeostasis (Yamashita et al., 2003).

Apart from its function in cell adhesion, Arm may also regulate Wg-dependent transcription of target genes in the testis. In support of this notion, we observed high levels of expression of an *in vivo* Wg transcriptional reporter Fz3RFP (Olson et al., 2011) in CySCs/early somatic cyst cells (Fig. 5A,A′, somatic lineage stained for *eya*). As has been reported previously, we noted that Wg appears to be specifically transcribed in somatic cells in the vicinity of the hub, and its expression gradually decreases as cells move away from the hub (Fig. 5B,B′) (Leatherman and DiNardo, 2008). Notably, the expression of the Fz3RFP reporter was markedly elevated in d59/d59 testes, especially in the somatic cyst cells that are associated with poorly differentiated germ cell clusters (yellow arrowheads in Fig. 5D,D′), compared with reporter expression in heterozygous sibling control flies (Fig. 5C,C′). Ectopic expression of the Fz3RFP reporter was also detected in d59/d59 germ cells, albeit to a much weaker extent (white arrowheads in Fig. 5D′). These data are consistent with a putative function of the miR-310/13 cluster in directly modulating or buffering Wg signaling activity in the *Drosophila* testis.

Next, we explored whether the miR-310/13 deletion phenotype was functionally dependent on increased activity of the Wg pathway in the *Drosophila* testis. Indeed, removal of one copy of each of the two Frizzled receptors (termed *fzfz2*), a manipulation shown to inhibit Arm-mediated Wg signaling (Chen and Struhl, 1999), in d59/d59 flies largely restored normal germ cell differentiation and morphology, although the accumulation of somatic cyst cells persisted (supplementary material Fig. S3D-D‴). Consistent with the morphological rescue, the fertility of these flies also appeared to be partially, but significantly, restored (supplementary material Fig. S3E).

To determine whether miR-310/13 regulation of the Wg pathway is required in the somatic or germ lineage, we expressed either cDNAs or shRNAs directed toward Wg pathway components using drivers for either lineage (Fig. 5; supplementary material Fig. S3). To address whether the d59/d59 phenotype was a consequence of elevated Arm levels, we depleted Arm in the somatic lineage either by expressing AxinGFP (Fig. 5E,E′) or an shRNA against *arm* (Fig. 5G,G′) under the control of C587-GAL4. Somatic overexpression of AxinGFP and RNAi-mediated knockdown of Arm led to a significant rescue of both germ cell differentiation and accumulation of Tj^+ cyst cells in the d59/d59 mutant testes (Fig. 5E,G), indicating that forced reduction of Arm protein levels in the soma of miR-310/13-deleted testes can restore WT testis morphology. RNAi-mediated depletion of E-cad using C587-GAL4 also rescued the abnormal germ cell accumulations (Fig. 5I,I′), albeit to a lesser extent (compare Fig. 5E,G with 5I). Control testes expressing the aforementioned transgenic constructs alone did not display any discernible phenotypes (supplementary material Fig. S3A-C′). The expression of AxinGFP (Fig. 5F,F′) or of shRNA against *arm* (Fig. 5H,H′) or *E-cad* (Fig. 5J,J′) in d59/d59 testes under the germline-specific driver *nanos*-GAL4 (nos-GAL4) also resulted in a significant rescue of the accumulation of undifferentiated germ cell clusters and somatic cyst cells.

The genetic interaction data suggest that the miR-310/13 LOF phenotype might be attributable to an elevation in Arm function in nuclear signaling and cell adhesion. Our observation that loss of Arm or E-cad in either cell lineage rescued the d59/d59 phenotype supports the notion that cell-cell contacts, in addition to Arm-mediated signaling, might be important for the regulation of proliferation/differentiation in both lineages. To test this, we co-expressed activated Arm in both early somatic (Tj-GAL4) and germ cells (nos-GAL4). Strikingly, we observed that Arm expression in both lineages can result in the formation of ectopic germ cell clusters that are associated with a distinct set of Tj^+ CySC/early cyst cells (Fig. 5K-K‴), which is somewhat reminiscent of the phenotypes observed in miR-310/13-deleted testes. These clusters resembled an ectopic hub surrounded by germ cells (two-cell clusters are marked with yellow dashed lines in Fig. 5K′) and Tj^+ somatic cells (Fig. 5K″). However, we did not observe a specific hub structure within these ectopic clusters.

The idea that cell adhesion might impact germ and somatic cell differentiation is particularly exciting. Since somatic cells can non-autonomously affect the differentiation program of the germ cells they envelop (Leatherman and DiNardo, 2008; Lim and Fuller, 2012; Tran et al., 2000; Voog et al., 2008), germ cell differentiation may be regulated by means of modulating adhesive interactions between germ and somatic cells. Based on the observation that miR-310/13-deficient testes exhibit a striking accumulation of $Zfh1^+$ early cyst progenitor cells, and that downregulation of components of cell adhesion and/or signaling in either lineage can at least partly rescue the phenotype, we propose that somatic support cells may non-autonomously influence germ cell differentiation by modulating both cell adhesion and signaling (see working model in Fig. 6; supplementary material Fig. S4). It is possible that increased Arm levels or activity promotes greater cell-cell adhesion between the somatic cyst cells that encapsulate the germ cells, as evidenced by robust and extensive electron-dense ‘adhesion-like’ structures observed in transmission electron microscopy images of d59/d59 versus WT testis (supplementary material Fig. S4). This in turn could prevent the germ cells from exiting the ‘extended niche’ provided by the increased number of $Zfh1^+$ CySC/early cyst cells, which instead continue to undergo TA divisions.

To investigate the Pan-dependent signaling functions of Arm in the germ and somatic cell lineages, we expressed shRNA directed against *pan* using either nos-GAL4 or C587-GAL4 in d59/d59 testis (supplementary material Fig. S3M-N′). The results revealed that whereas Pan knockdown under nos-GAL4 significantly rescued germ cell differentiation (supplementary material Fig. S3N,N′), its knockdown in the somatic lineage had a minimal effect on the germ cell clustering phenotype (supplementary material Fig. S3M,M′). These data suggest a prominent function for Pan-mediated nuclear signaling of Arm in the germ lineage. The phenotypes observed in the somatic lineage might be reflective of Arm function in cell adhesion, perhaps via E-cad (supplementary material Fig. S4). These results concur with the genetic interaction we observed with *fzfz2*, where the reduction of FzFz2 levels resulted in the rescue of germ cell differentiation but did not appear to significantly rescue the somatic cell phenotype (increased Tj^+ cells in supplementary material Fig. S3D″), corroborating the hypothesis that the Pan-dependent activity of Arm might have a more prominent function in germ cells.

Taken together, these observations suggest that miR-310/13 might function to fine-tune cell signaling and adhesion activities in both lineages by modulating the levels/activity of Arm, thereby

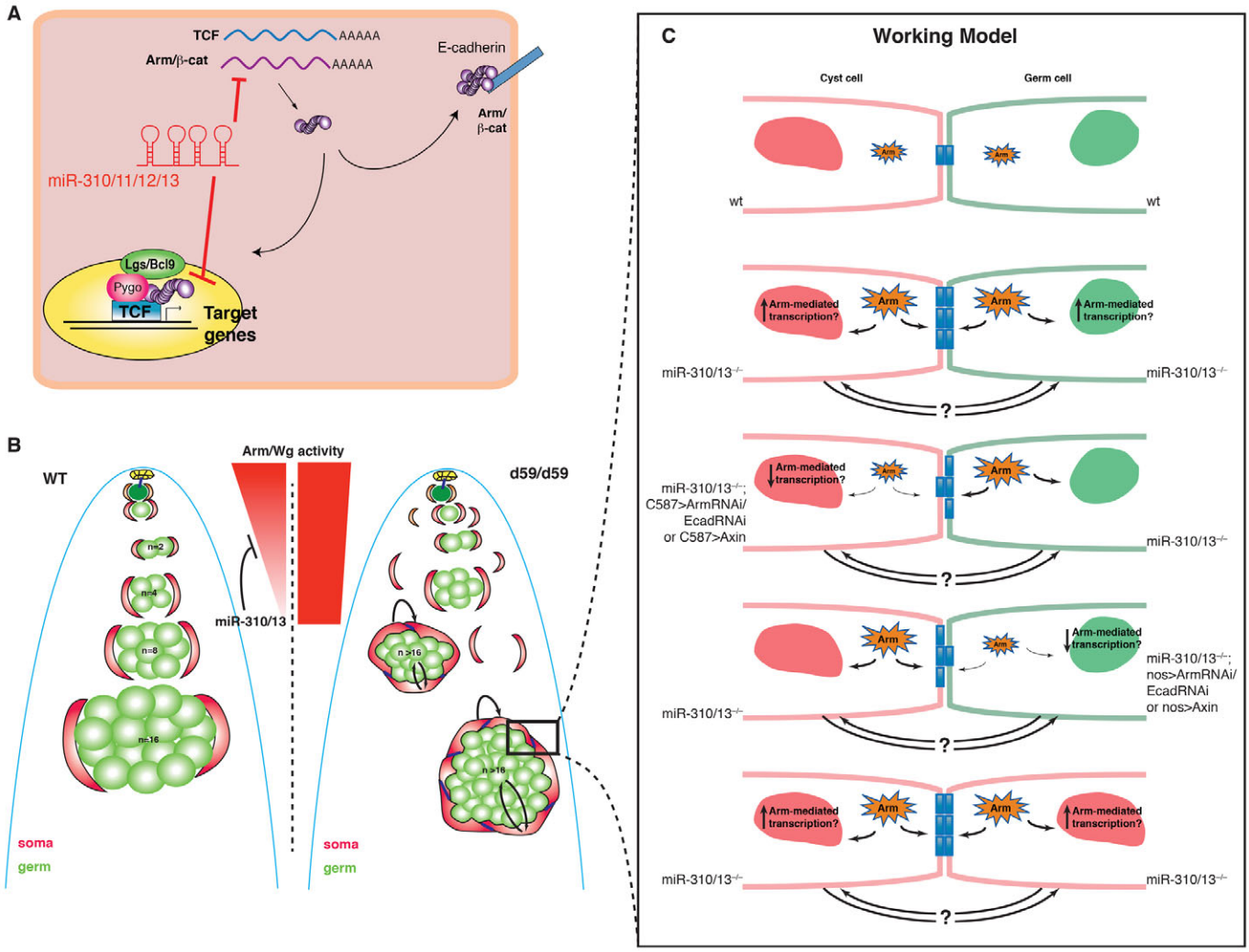

Fig. 6. Model for miR-310/13 regulation of Arm function. (**A**) Components of the miR-310/13 cluster may directly target the mRNA for Arm/β-cat and/or Pan/TCF, modulating their levels. miRNA-mediated modulation of Arm levels can result in changes in transcription of target genes and in cell-cell adhesion. (**B**) Model representing the phenotype observed in miR-310/13-deficient testis (right) compared with WT testes (left). Poorly differentiated germ cell clusters (green) are enveloped by an increased number of somatic cyst cells (red). Arrows depict putative signaling interactions between germ cells and soma. We propose that high levels of Wg/Arm activity, and additional signaling interactions between the expanded soma and the associated germ cells, maintain the germ cells in early stages of differentiation. Moreover, the miR-310/13 cluster may function to diminish Arm activity/expression in order to facilitate further steps in the differentiation and maturation of germ and cyst somatic cells. (**C**) Model for the cellular mechanisms that might influence the miR-310/13 mutant phenotype. Deletion of miR-310/13 may lead to increased levels of cytosolic Arm, which can modulate both transcription of target genes and the strength of cell-cell contacts (see supplementary material Fig. S4). Increased transcription could potentially affect the proliferative state of either somatic or germline cells in a cell-autonomous or non-autonomous fashion. Modulation of cell adhesion could also perturb the differentiation process non-autonomously. Supporting this model is the observation that reduction in Arm or E-cad levels in either cell lineage leads to rescue of the abnormal germ cell accumulation phenotype (Fig. 5; supplementary material Fig. S3).

facilitating the proper differentiation program in early germ and somatic cyst cells.

DISCUSSION

The current paradigm regarding the conserved function of Wnts in metazoans involves a highly regulated dosage of Wnt pathway activity, with too little or too much leading to abnormal cellular changes and diseases such as cancer. Through their ability to fine-tune protein levels, miRNAs are ideal candidates to refine the gradient of the Wnt response characteristic of numerous developmental contexts (van Amerongen and Nusse, 2009). In this study, we describe the identification of the miR-310/13 cluster and its human ortholog hsa-miR-25 as a conserved antagonist of the Wnt/Wg signaling pathway. Our results suggest that the miR-310/13 cluster can modulate Wg signaling activity by directly targeting the *arm* and *pan* 3′-UTRs. We show that misexpression of miR-310/13 within clones can modulate endogenous Arm levels (Fig. 2H′). We also demonstrate that *in vivo* overexpression of miR-310 can phenocopy Arm/Wg LOF phenotypes in wing and leg imaginal discs, and that co-expression of *arm* cDNA lacking its 3′-UTR can rescue the miR-310/13 misexpression phenotype.

In addition to its previously reported role in neuronal synapses at neuromuscular junctions (Tsurudome et al., 2010), we have uncovered a novel function of miR-310/13 in the regulation of germ

and somatic cell homeostasis in the *Drosophila* testis. LOF phenotypes of miR-310/13 in the male gonad revealed a crucial function for miRNA-mediated regulation of Wg/Arm activity in the control of normal differentiation and/or proliferation in both somatic and germ cell lineages. Specifically, we demonstrate that: (1) Wg-lacZ is expressed in CySCs and early cyst somatic cells, thereby suggesting a function for Arm/Wg activity in the regulation of germ and cyst cell differentiation (Fig. 5B′) (Leatherman and DiNardo, 2008); (2) Fz3RFP reporter expression is markedly upregulated in miR-310/13-deficient testes (Fig. 5D′); (3) there is a significant increase in the number of Zfh1$^+$ Tj$^+$ CySC/early cyst cells (Fig. 4G‴,I; supplementary material Fig. S2F) and a striking accumulation of large, poorly differentiated, early germ cell clusters in miR-310/13-deficient testes (Fig. 4G′; supplementary material Fig. S2H′); (4) the miR-310/13 LOF phenotype can be significantly rescued by inhibition of Arm levels/activity; and (5) simultaneous misexpression of Arm in both germ and somatic lineages can somewhat recapitulate the miR-310/13-deficient phenotype in the *Drosophila* testis (Fig. 5K-K‴).

We note that the differences in the phenotypes of Arm overexpression in both lineages compared with miR-310/13 LOF could result from a variety of factors, including the use of lineage-specific drivers that are spatially/temporally regulated versus a complete LOF phenotype, and the changes in the levels of Arm and/or Pan (as *pan* also appears to be regulated by miR-310/13, Fig. 1) in *arm* transgenic versus miR-deleted testes. In spite of the differences in phenotype, the important similarity is that the ectopic germ cell clusters in Arm-expressing testes appear to be restricted to an early stage of differentiation (Fig. 5K′), similar to what we observe in the miR-310/13-deleted flies (Fig. 4G). Additionally, it has previously been shown that Bam expression levels determine the number of TA mitotic divisions, thus regulating proliferation/differentiation in the adult germ cell lineage. Bam is not expressed in two-cell cysts, but its expression increases in four- to eight-cell cysts and drastically drops after the 16-cell stage (Gönczy et al., 1997; Insco et al., 2009). These results, together with our observation that the differentiation marker Bam is either very low or completely absent in the large germ cell clusters, their inability to exit the cell cycle and that they display compact nuclear morphology in miR-310/13-deficient testes, are consistent with the notion that ectopic increases in Arm activity can result in the failure of differentiation of germ cells beyond the two- to early four-cell cyst.

Intriguingly, the germ cell clustering phenotype in d59 mutants is somewhat reminiscent of reduced TGFβ signaling activity. The main difference, however, is that whereas Bam expression is robustly upregulated in *saxophone* (*sax*) mutant (TGFβ signaling-deficient) testis (Li et al., 2007), it was absent or undetectable in d59/d59 mutants (supplementary material Fig. S2H′). Previous reports have indicated that BMP ligands, such as Dpp and Gbb, secreted from the hub and CySCs are required to inhibit differentiation of GSCs by inhibiting Bam expression (DiNardo et al., 2011; Flaherty et al., 2010; Li et al., 2007). Moreover, once Bam expression is turned off, TGFβ signaling is no longer required for the continued proliferation of the germ cells (DiNardo et al., 2011). We evaluated the levels of phosphorylated Mad (p-Mad) as a readout for TGFβ signaling in the d59 mutant testes. We noted an increase in the number of p-Mad$^+$ early germ cells and cyst cells (white and blue arrowheads, respectively, supplementary material Fig. S5B,B′) compared with WT testis (supplementary material Fig. S5A,A′). However, p-Mad immunostaining was undetectable in the large abnormal germ cell clusters (yellow arrowheads in supplementary material Fig. S5B,B′; *n*=20). We postulate that the increased number of Tj$^+$, and in many cases Zfh1$^+$, early cyst cells is a consequence of dysregulated Arm/Wg activity, which in turn prevents differentiation of the associated germ cells [perhaps by activating TGFβ signaling in the early germ cells (DiNardo et al., 2011)]. However, the sustained proliferation observed in the germ cell clusters in d59/d59 mutants is likely to be due to increased Pan-dependent Arm signaling, as judged by the marked rescue of the clustering phenotype in testis knocked down for Pan function (supplementary material Fig. S3N,N′). We postulate that Wg-mediated control of Arm levels or activity might have important functions in the proliferation and differentiation of both somatic and germ cells, and that the fine-tuning of Arm activity by miR-310/13 might serve as an important mechanism to control the robust and stereotypical program of proliferation and differentiation of germ and somatic lineage progenitors in the *Drosophila* testis.

Finally, multiple studies suggest that the cytosolic availability of β-cat can be influenced by the abundance of E-cad, which has been shown to sequester transcriptionally prone β-cat to the plasma membrane (Cox et al., 1996; Fagotto et al., 1996). In stem cell maintenance or tumor establishment, the equilibrium between β-cat-mediated adhesion and transcription is synonymous to homeostasis or cancer progression. Recent evidence from studies in embryonic stem cells (ESCs) also suggests crucial functions of cell adhesion through cadherin-catenin complexes in stem cell homeostasis (Lyashenko et al., 2011). We propose that miRNAs such as miR-310/13 may regulate the Wnt response by modulating not only gene transcription, but also cell-cell adhesion. Such miRNA modulation of β-cat function in cellular adhesion might represent a previously unexplored mechanism of stem cell maintenance and differentiation.

Acknowledgements
We thank Dr Chi Yun and Shauna Katz at the NYU RNAi Core Facility (supported by the NYU Cancer Institute and the Kimmel Center for Stem Cell Biology) for screening support during the primary miRNA screen; Dr Nicholas Tolwinski for the UAS-AxinGFP fly stock; Dr Norbert Perrimon for the UAS-RNAi (TRiP) lines; and Dr Alfonso Martinez-Arias for critical reading of the manuscript.

Funding
This work was partially supported by the March of Dimes [Research Grant #FY10-363] and American Cancer Society [Research Scholar Grant #RSG-11-108-01-CDD]. Work in the E.C.L. group was supported by the National Institutes of Health (NIH) [R01-GM083300]. TRiP at Harvard Medical School is funded by the NIH/National Institute of General Medical Sciences (NIGMS) [R01-GM084947]. Deposited in PMC for release after 12 months.

Competing interests statement
The authors declare no competing financial interests.

Author contributions
R.P., M.S.F. and R.D. conceived and designed the experiments. R.P., F.P., C.G.-G., A.J.K., E.R.O., F.-X.L., J.-S.Y., M.S.F. and R.D. performed the experiments. R.P., F.P., M.S.F. and R.D. analyzed the data. P.S., J.-S.Y., E.C.L. and R.D. contributed reagents/materials/analysis tools. R.P., F.P., M.S.F. and R.D. wrote the manuscript.

Supplementary material
Supplementary material available online at
http://dev.biologists.org/lookup/suppl/doi:10.1242/dev.092817/-/DC1

References

Anton, R., Chatterjee, S. S., Simundza, J., Cowin, P. and Dasgupta, R. (2011). A systematic screen for micro-RNAs regulating the canonical Wnt pathway. *PLoS ONE* **6**, e26257.
Basler, K. and Struhl, G. (1994). Compartment boundaries and the control of Drosophila limb pattern by hedgehog protein. *Nature* **368**, 208-214.

Brennan, K., Gonzalez-Sancho, J. M., Castelo-Soccio, L. A., Howe, L. R. and Brown, A. M. (2004). Truncated mutants of the putative Wnt receptor LRP6/Arrow can stabilize beta-catenin independently of Frizzled proteins. *Oncogene* **23**, 4873-4884.
Bushati, N. and Cohen, S. M. (2007). microRNA functions. *Annu. Rev. Cell Dev. Biol.* **23**, 175-205.
Calin, G. A. and Croce, C. M. (2006). MicroRNA signatures in human cancers. *Nat. Rev. Cancer* **6**, 857-866.
Chen, D. and McKearin, D. (2003). Dpp signaling silences bam transcription directly to establish asymmetric divisions of germline stem cells. *Curr. Biol.* **13**, 1786-1791.
Chen, C. M. and Struhl, G. (1999). Wingless transduction by the Frizzled and Frizzled2 proteins of Drosophila. *Development* **126**, 5441-5452.
Cox, R. T., Kirkpatrick, C. and Peifer, M. (1996). Armadillo is required for adherens junction assembly, cell polarity, and morphogenesis during Drosophila embryogenesis. *J. Cell Biol.* **134**, 133-148.
Croce, C. M. (2009). Causes and consequences of microRNA dysregulation in cancer. *Nat. Rev. Genet.* **10**, 704-714.
DasGupta, R., Kaykas, A., Moon, R. T. and Perrimon, N. (2005). Functional genomic analysis of the Wnt-wingless signaling pathway. *Science* **308**, 826-833.
DasGupta, R., Nybakken, K., Booker, M., Mathey-Prevot, B., Gonsalves, F., Changkakoty, B. and Perrimon, N. (2007). A case study of the reproducibility of transcriptional reporter cell-based RNAi screens in Drosophila. *Genome Biol.* **8**, R203.
DiNardo, S., Okegbe, T., Wingert, L., Freilich, S. and Terry, N. (2011). lines and bowl affect the specification of cyst stem cells and niche cells in the Drosophila testis. *Development* **138**, 1687-1696.
Easwaran, V., Song, V., Polakis, P. and Byers, S. (1999). The ubiquitin-proteasome pathway and serine kinase activity modulate adenomatous polyposis coli protein-mediated regulation of beta-catenin-lymphocyte enhancer-binding factor signaling. *J. Biol. Chem.* **274**, 16641-16645.
Estella, C. and Mann, R. S. (2008). Logic of Wg and Dpp induction of distal and medial fates in the Drosophila leg. *Development* **135**, 627-636.
Fagotto, F., Funayama, N., Gluck, U. and Gumbiner, B. M. (1996). Binding to cadherins antagonizes the signaling activity of beta-catenin during axis formation in Xenopus. *J. Cell Biol.* **132**, 1105-1114.
Flaherty, M. S., Salis, P., Evans, C. J., Ekas, L. A., Marouf, A., Zavadil, J., Banerjee, U. and Bach, E. A. (2010). chinmo is a functional effector of the JAK/STAT pathway that regulates eye development, tumor formation, and stem cell self-renewal in Drosophila. *Dev. Cell* **18**, 556-568.
Goentoro, L. and Kirschner, M. W. (2009). Evidence that fold-change, and not absolute level, of beta-catenin dictates Wnt signaling. *Mol. Cell* **36**, 872-884.
Gönczy, P., Matunis, E. and DiNardo, S. (1997). bag-of-marbles and benign gonial cell neoplasm act in the germline to restrict proliferation during Drosophila spermatogenesis. *Development* **124**, 4361-4371.
Hoffmans, R., Städeli, R. and Basler, K. (2005). Pygopus and legless provide essential transcriptional coactivator functions to armadillo/beta-catenin. *Curr. Biol.* **15**, 1207-1211.
Hülsken, J., Birchmeier, W. and Behrens, J. (1994). E-cadherin and APC compete for the interaction with beta-catenin and the cytoskeleton. *J. Cell Biol.* **127**, 2061-2069.
Hutvagner, G. and Zamore, P. D. (2002). A microRNA in a multiple-turnover RNAi enzyme complex. *Science* **297**, 2056-2060.
Insco, M. L., Leon, A., Tam, C. H., McKearin, D. M. and Fuller, M. T. (2009). Accumulation of a differentiation regulator specifies transit amplifying division number in an adult stem cell lineage. *Proc. Natl. Acad. Sci. USA* **106**, 22311-22316.
Issigonis, M. and Matunis, E. (2012). The Drosophila BCL6 homolog Ken and Barbie promotes somatic stem cell self-renewal in the testis niche. *Dev. Biol.* **368**, 181-192.
Kennell, J. A., Gerin, I., MacDougald, O. A. and Cadigan, K. M. (2008). The microRNA miR-8 is a conserved negative regulator of Wnt signaling. *Proc. Natl. Acad. Sci. USA* **105**, 15417-15422.
Kiger, A. A. and Fuller, M. T. (2001). Male germ-line stem cells. In *Stem Cell Biology* (ed. D. R Marshak, R. L. Gardner and D. Gottlieb), pp.149-188. Cold Spring Harbor, NY: Cold Spring Harbor Laboratory Press.
Leatherman, J. L. and DiNardo, S. (2008). Zfh-1 controls somatic stem cell self-renewal in the Drosophila testis and nonautonomously influences germline stem cell self-renewal. *Cell Stem Cell* **3**, 44-54.
Leatherman, J. L. and DiNardo, S. (2010). Germline self-renewal requires cyst stem cells and stat regulates niche adhesion in Drosophila testes. *Nat. Cell Biol.* **12**, 806-811.
Lee, T. and Luo, L. (2001). Mosaic analysis with a repressible cell marker (MARCM) for Drosophila neural development. *Trends Neurosci.* **24**, 251-254.
Li, M. A., Alls, J. D., Avancini, R. M., Koo, K. and Godt, D. (2003). The large Maf factor Traffic Jam controls gonad morphogenesis in Drosophila. *Nat. Cell Biol.* **5**, 994-1000.
Li, C. Y., Guo, Z. and Wang, Z. (2007). TGFbeta receptor saxophone non-autonomously regulates germline proliferation in a Smox/dSmad2-dependent manner in Drosophila testis. *Dev. Biol.* **309**, 70-77.
Lim, J. G. and Fuller, M. T. (2012). Somatic cell lineage is required for differentiation and not maintenance of germline stem cells in Drosophila testes. *Proc. Natl. Acad. Sci. USA* **109**, 18477-18481.
Lin, H., Yue, L. and Spradling, A. C. (1994). The Drosophila fusome, a germline-specific organelle, contains membrane skeletal proteins and functions in cyst formation. *Development* **120**, 947-956.
Lindsley, D. T. and Tokuyasu, K. T. (1980). Spermatogenesis. In *Genetics and Biology of Drosophila* (ed. M. Ashburner and T. R. F. Wright), pp. 225-294. New York, NY: Academic Press.
Lyashenko, N., Winter, M., Migliorini, D., Biechele, T., Moon, R. T. and Hartmann, C. (2011). Differential requirement for the dual functions of β-catenin in embryonic stem cell self-renewal and germ layer formation. *Nat. Cell Biol.* **13**, 753-761.
Martinez, J. and Tuschl, T. (2004). RISC is a 5′ phosphomonoester-producing RNA endonuclease. *Genes Dev.* **18**, 975-980.
McKearin, D. M. and Spradling, A. C. (1990). bag-of-marbles: a Drosophila gene required to initiate both male and female gametogenesis. *Genes Dev.* **4** 12B, 2242-2251.
Morrison, S. J. and Spradling, A. C. (2008). Stem cells and niches: mechanisms that promote stem cell maintenance throughout life. *Cell* **132**, 598-611.
Nolo, R., Abbott, L. A. and Bellen, H. J. (2001). Drosophila Lyra mutations are gain-of-function mutations of senseless. *Genetics* **157**, 307-315.
Nusse, R. (2005). Wnt signaling in disease and in development. *Cell Res.* **15**, 28-32.
Olson, E. R., Pancratov, R., Chatterjee, S. S., Changkakoty, B., Pervaiz, Z. and DasGupta, R. (2011). Yan, an ETS-domain transcription factor, negatively modulates the Wingless pathway in the Drosophila eye. *EMBO Rep.* **12**, 1047-1054.
Pai, L. M., Orsulic, S., Bejsovec, A. and Peifer, M. (1997). Negative regulation of Armadillo, a Wingless effector in Drosophila. *Development* **124**, 2255-2266.
Peifer, M., Rauskolb, C., Williams, M., Riggleman, B. and Wieschaus, E. (1991). The segment polarity gene armadillo interacts with the wingless signaling pathway in both embryonic and adult pattern formation. *Development* **111**, 1029-1043.
Polakis, P. (2000). Wnt signaling and cancer. *Genes Dev.* **14**, 1837-1851.
Reich, J., Snee, M. J. and Macdonald, P. M. (2009). miRNA-dependent translational repression in the Drosophila ovary. *PLoS ONE* **4**, e4669.
Saydam, O., Shen, Y., Würdinger, T., Senol, O., Boke, E., James, M. F., Tannous, B. A., Stemmer-Rachamimov, A. O., Yi, M., Stephens, R. M. et al. (2009). Downregulated microRNA-200a in meningiomas promotes tumor growth by reducing E-cadherin and activating the Wnt/beta-catenin signaling pathway. *Mol. Cell. Biol.* **29**, 5923-5940.
Schnall-Levin, M., Zhao, Y., Perrimon, N. and Berger, B. (2010). Conserved microRNA targeting in Drosophila is as widespread in coding regions as in 3′UTRs. *Proc. Natl. Acad. Sci. USA* **107**, 15751-15756.
Silver, S. J., Hagen, J. W., Okamura, K., Perrimon, N. and Lai, E. C. (2007). Functional screening identifies miR-315 as a potent activator of Wingless signaling. *Proc. Natl. Acad. Sci. USA* **104**, 18151-18156.
Struhl, G. and Basler, K. (1993). Organizing activity of wingless protein in Drosophila. *Cell* **72**, 527-540.
Tanzer, A. and Stadler, P. F. (2004). Molecular evolution of a microRNA cluster. *J. Mol. Biol.* **339**, 327-335.
Thatcher, E. J., Paydar, I., Anderson, K. K. and Patton, J. G. (2008). Regulation of zebrafish fin regeneration by microRNAs. *Proc. Natl. Acad. Sci. USA* **105**, 18384-18389.
Tolwinski, N. S., Wehrli, M., Rives, A., Erdeniz, N., DiNardo, S. and Wieschaus, E. (2003). Wg/Wnt signal can be transmitted through arrow/LRP5,6 and Axin independently of Zw3/Gsk3beta activity. *Dev. Cell* **4**, 407-418.
Tran, J., Brenner, T. J. and DiNardo, S. (2000). Somatic control over the germline stem cell lineage during Drosophila spermatogenesis. *Nature* **407**, 754-757.
Tsurudome, K., Tsang, K., Liao, E. H., Ball, R., Penney, J., Yang, J. S., Elazzouzi, F., He, T., Chishti, A., Lnenicka, G. et al. (2010). The Drosophila miR-310 cluster negatively regulates synaptic strength at the neuromuscular junction. *Neuron* **68**, 879-893.
Tulina, N. and Matunis, E. (2001). Control of stem cell self-renewal in Drosophila spermatogenesis by JAK-STAT signaling. *Science* **294**, 2546-2549.
van Amerongen, R. and Nusse, R. (2009). Towards an integrated view of Wnt signaling in development. *Development* **136**, 3205-3214.
Voog, J., D'Alterio, C. and Jones, D. L. (2008). Multipotent somatic stem cells contribute to the stem cell niche in the Drosophila testis. *Nature* **454**, 1132-1136.
Widmann, T. J. and Dahmann, C. (2009). Wingless signaling and the control of cell shape in Drosophila wing imaginal discs. *Dev. Biol.* **334**, 161-173.
Yamashita, Y. M., Jones, D. L. and Fuller, M. T. (2003). Orientation of asymmetric stem cell division by the APC tumor suppressor and centrosome. *Science* **301**, 1547-1550.